A PARAMETRIC STUDY ON THE INFLUENCE OF THE NONLINEAR CHARACTERISTICS OF THE SECONDARY SUSPENSION UPON THE VERTICAL VIBRATIONS IN THE RAILWAY VEHICLES

Mădălina DUMITRIU[1]

The paper herein regards to a parametric study aiming to evaluate the influence of the nonlinear characteristics of the secondary suspension upon the behaviour of vertical vibrations of the railway vehicle. The nonlinearity of the secondary suspension model is given by the component of the elastic force and the component of the dry friction force. The study is based on the results from the numerical simulation of the free vibrations behaviour, the steady-state harmonic behaviour of vibrations and of the random vibrations behaviour. A series of properties of the non-linear system have been pointed out at and the selective influence of the dry friction force has been proven, as a function of the excitation frequency and the carbody reference point. Similarly, it has been drawn attention to the influence of the dry friction force upon the ride quality and ride comfort of the railway vehicle.

Keywords: railway vehicle, suspension, coil spring - rubber, non-linear model, vibration behaviour

1. Introduction

During running, the railway vehicle is subjected to a permanent behaviour of vibrations, with inconvenient effects on the ride quality, ride comfort and safety, whose main cause is to be found in the interaction between the vehicle and the track (Cheli and Corradi, 2011; Mazilu, 2009; Young et al., 2003).

The evaluation of the vibrations behaviour in the vehicle is already done in the designing stage, in order to optimize the dynamic performance of the vehicle and, at a later date, to investigate the issues emerging during exploitation, when using for this purpose programs of numerical simulation developed on the basis of theoretical models of the vehicle (Evans and Berg, 2009; Schupp, 2003). The ‚virtual homologation' of the railway vehicles also requires tests based on numerical models and virtual simulations (Funfschilling et al., 2012; Jönsson et al., 2008).

The suspension plays an important role in terms of the capacity of the passenger trains to provide, at least for the level of vibrations, ride quality and ride comfort. The potential and success of the numerical simulations to evaluate the vibrations behaviour of the vehicle greatly depend on how the suspension components are modelled (Eickhoff et al., 1995; Bruni et al, 2011). Quality and

[1] Department of Railway Vehicles, University Politehnica of Bucharest, Romania
e-mail: madalinadumitriu@yahoo.com

even quantity-based results can be obtained from simple models, where the suspension components are considered to have linear characteristics. For instance, the rubber elements that are frequently used in the railway engineering both for the vehicle suspension and the track superstructure, are modelled via Kelvin-Voigt systems (Mazilu, 2010). The use of such models can, however, lead to results of the numerical simulations with a low degree of feasibility and reliability.

The goal of this paper is focused on the analysis of the influence that the nonlinear characteristics of the suspension have upon the vertical vibrations in the railway vehicles. To this purpose, a passenger coach was considered, one that includes in its secondary suspension a mix coil spring – rubber and it is represented by an original model (Dumitriu, 2016). The model for the mix coil spring – rubber is developed on the basis of a non-linear dynamic rubber spring model (Berg, 1997, 1998), which best reflects the mechanical behaviour of rubber suspension components in railway vehicle dynamics and also provides a very good agreement between the theoretical and experimental results. The model in this paper, similar with the initial one, relies on the overlapping of three component forces, working in parallel – the elastic force, viscous force and friction force. Unlike the initial model, this one has its elastic component represented by an elastic element with a graded variable stiffness, which includes both the elastic force in the coil spring and the one in the rubber element. The model carries two sources of nonlinearity, one coming from the component of the friction force and the other from the component of the elastic force.

The nonlinear model of the secondary suspension is embodied in the vehicle model, which is a rigid-flexible coupled type model. The carbody is modelled as free-free Euler-Bernoulli equivalent beam, where this model allows considering the first bending mode of the carbody that has a significant importance on the vertical vibrations behaviour of the carbody (Diana et al., 2002).

The study is based on the results from the numerical simulation of the free vibrations behaviour the steady-state harmonic behaviour of vibrations and of the random vibrations behaviour and on the evaluation of the level of vertical vibrations in three reference points of the carbody – at the centre and above the bogies, depending on the component of the dry friction force developed in the rubber element.

2. The mechanical model of the vehicle

Fig. 1 shows the mechanical model of a four-wheelset, two-level suspension vehicle, which travels at a constant velocity V on a track that is considered perfectly rigid, with vertical irregularities. The track irregularities are described

against each wheelset by the functions $\eta_{j,(j+1)}$, with $j = 2i\text{-}1$, for $i = 1, 2$, while mentioning that every bogie i is fitted with the axles j and j+1.

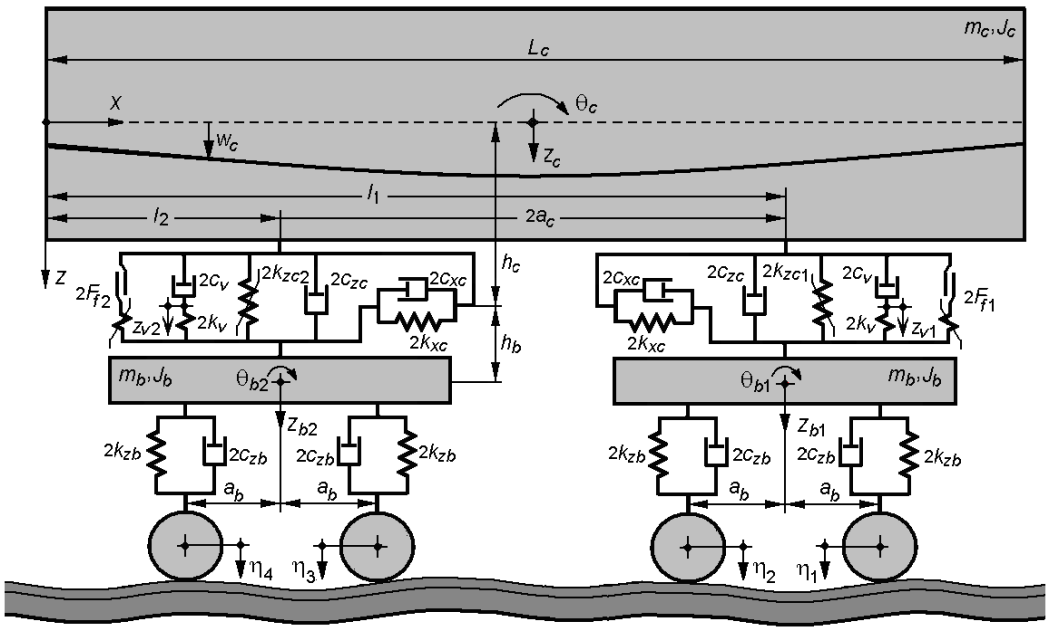

Fig. 1. The vehicle mechanical model.

The carbody is represented by a free-free equivalent beam, with constant cross-section and uniformly distributed mass, of Euler-Bernoulli type. The beam parameters are defined in terms of the carbody, such as: L_c – beam length; $\rho_c = m_c/L_c$ – beam mass per length unit, where m_c is the carbody mass; μ - structural damping coefficient; EI – bending modulus, where E is the longitudinal modulus of elasticity, and I is the area moment of inertia of the beam cross-section.

There will be taken into account the carbody rigid vibration modes - bounce z_c and pitch θ_c, and the first carbody natural bending mode in a vertical plan – symmetrical bending. The carbody inertia reported to the rigid vibration modes is represented by mass m_c and the mass moment of inertia J_c. The carbody wheelbase is $2a_c$. Distances $l_{1,2} = L_c/2 \pm a_c$ fix the supporting points position of the carbody on the secondary suspension.

The carbody vertical movement $w_c(x,t)$ comes from the superposition of the two rigid vibration modes with the first bending mode

$$w_c(x,t) = z_c(t) + \left(x - \frac{L_c}{2} \right) \theta_c(t) + X_c(x) T_c(t), \tag{2.1}$$

where $T_c(t)$ is the time coordinate of the first natural bending mode in a vertical plan and $X_c(x)$ stands for its eigenfunction

$$X_c(x) = \sin\beta x + \sinh\beta x - \frac{\sin\beta L_c - \sinh\beta L_c}{\cos\beta L_c - \cosh\beta L_c}(\cos\beta x + \cosh\beta x), \tag{2.2}$$

$$\text{with} \qquad \beta = \sqrt[4]{\omega_c^2 \rho_c / (EI)}\ ,\ \cos\beta L_c \cosh\beta L_c - 1 = 0, \tag{2.3}$$

where ω_c is the natural angular frequency of the carbody symmetrical bending.

The stiffness, damping and the modal mass of the carbody are given by the equations below

$$k_{mc} = EI\int_0^L \left(\frac{\mathrm{d}^2 X_c}{\mathrm{d}x^2}\right)^2 \mathrm{d}x\ ;\ c_{mc} = \mu I\int_0^L \left(\frac{\mathrm{d}^2 X_c}{\mathrm{d}x^2}\right)^2 \mathrm{d}x\ ;\ m_{mc} = \rho_c \int_0^L X_c^2 \mathrm{d}x\ . \tag{2.4}$$

The bogies have two degrees of freedom, namely bounce z_{bi} and pitch θ_{bi}, with $i = 1, 2$. Each bogie has the mass m_b, inertia moment J_b and wheelbase $2a_b$.

The elastic mix of the secondary suspension pertinent to a bogie is represented by a unidimensional nonlinear model, comprising of three components operating in parallel (Dumitriu, 2016): an elastic element of variable stiffness $2k_{zc1,2}$; a Maxwell system that includes an element of viscous damping of a constant $2c_v$ in series with an elastic element of stiffness $2k_v$; an elastic element in series with a friction element that help with the modelling of the component of the friction force $2F_{f1,2}$. This model is used to represent the mix coil spring – rubber in the secondary suspension of the Y 32R bogie. The mix coil spring-rubber model will be described in the next section. The damping of the secondary suspension is taken into account by the damping constant $2c_{zc}$.

The plan of the secondary suspension finds at distance of h_c from the carbody medium fiber and at distance h_b from the bogie centre of gravity. The longitudinal traction system between carbody and bogie is shaped via a Kelvin-Voigt system with the elastic constant $2k_{xc}$ and damping constant $2c_{xc}$.

The vertical primary suspension corresponding to an axle is modelled by a Kelvin-Voigt system with the elastic constant $2k_{zb}$ and damping constant $2c_{zb}$.

3. The non-linear model of the mix coil spring-rubber

Figure 2 shows a mix coil spring - rubber used in the secondary suspension of the Y 32R which certain passenger railway vehicles are fitted with. The static characteristic of the mix in the vertical direction is featured in Fig. 3. This characteristic is noticed to be of a non-linear type with step-wise/graded variation of stiffness. The stiffness of the mix increases along with the applied loading, due to the rubber deformation.

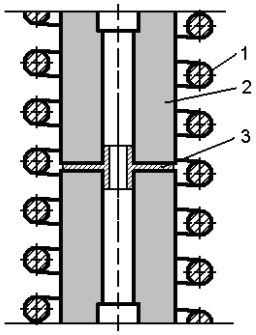

Fig. 2. Mix coil spring - rubber: 1. coil spring; 2. rubber; 3. intermediary element.

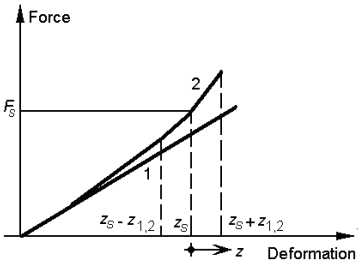

Fig. 3. The static characteristic: 1. the characteristic of the coil spring; 2. the characteristic of the mix coil spring - rubber.

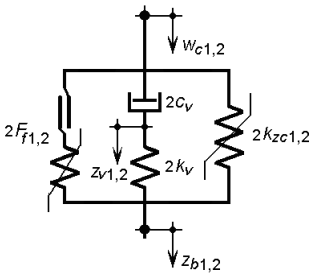

Fig. 4. Model for mix coil spring – rubber.

The proposed model to represent the mix coil spring – rubber is featured in Fig. 4 (Dumitriu, 2016). This model relies on Berg's model (Berg, 1997, 1998), which very well expresses the mechanical behaviour of rubber suspension components in railway vehicle dynamics.

The Berg model is a one-dimension model, based on the overlapping of three component forces working in parallel, where each of them contributes to the total deformation force of the rubber spring (Berg, 1997). They include the component of the elastic force, the viscous force and the dry friction component. The elastic force component is linear and models the rubber elasticity property. When introducing the viscous force, the increase in stiffness triggers a similar frequency response, as well as the rate-dependent hysteresis. The inclusion of a friction force means an increased stiffness at small displacement amplitudes as well as rate-independent hysteresis.

The mix coil spring - rubber model consists of the same three components operating in parallel (see. Fig. 4), as in Berg's model. The elastic force component is thus described by an elastic element that has a graded variable stiffness $2k_{zc1,2}$, unlike Berg's model. It includes both the elastic force in the coil spring and the other one in the rubber element.

The elastic force is calculated as a function of the direction of the relative displacement $z_{1,2}$ in relation to the equilibrium position of the system under the action of the static force F_s, while considering the variation in the stiffness of the elastic mix

$$F_{e1,2} = 2k_{zc1,2}z_{1,2}\,, \tag{3.1}$$

where $k_{zc1,2} = k_{zcc}$, for $z_{1,2} > 0$, and $k_{zc1,2} = k_{zcd}$, for $z_{1,2} < 0$, with $k_{zcc} > k_{zcd}$; k_{zcc} means the stiffness of the elastic mix during compression and k_{zcd} is the stiffness of the elastic mix during expansion. The relative displacement $z_{1,2}$ is

$$z_{1,2} = w_{c1,2} - z_{b1,2}\,, \tag{3.2}$$

where $w_{c1,2}$ is the vertical displacement of the carbody against the leaning points on the secondary suspension

$$w_{c1,2} = w_c(l_{1,2}) = z_c \pm a_c\theta_c + X_c(l_{1,2})T_c\,. \tag{3.3}$$

As for the viscous force component, this is represented by a Maxwell system containing an element of viscous damping of constant $2c_v$ in series with an elastic element of stiffness $2k_v$. The viscous force is determined as follows

$$F_{v1,2} = c_v(\dot{w}_{c1,2} - \dot{z}_{v1,2}) = k_v(z_{v1,2} - z_{b1,2})\,. \tag{3.4}$$

The component of the friction force is modelled as a 'smooth Coulomb friction force' to avoid the issues emerging during the numerical simulations due to the fact that Coulomb model is non-smooth, multi-valued and non-differentiable (Berg, 1997, 1998).

The friction force depends on the relative displacement $z_{1,2}$ of the system, as well as on the reference state ($z_{r1,2}$, $F_{fr1,2}$), that corresponds with the change in the sign of the relative speed $\dot{z}_{1,2}$. Two more parameters are defined, namely the maximum friction force $F_{f\max}$ and the relative displacement z_0 for which the friction force is half the value of the maximum friction force $F_{f1,2} = F_{f\max}/2$, when starting from the initial reference state ($z_{r1,2} = 0$, $F_{f1,2} = 0$) and reaching z_0.

The friction force is defined in relation to the reference state, as follows:

$$F_{f1,2} = F_{fr1,2}\text{, for } \; z_{1,2} = z_{r1,2}\,; \tag{3.5}$$

$$F_{f1,2} = F_{fr1,2} + \frac{z_{1,2} - z_{r1,2}}{z_0(1-\alpha_{1,2}) + (z_{1,2} - z_{r1,2})}(F_{f\max} - F_{fr1,2})\text{, for } z_{1,2} > z_{r1,2}; \tag{3.6}$$

$$F_{f1,2} = F_{fr1,2} + \frac{z_{1,2} - z_{r1,2}}{z_0(1+\alpha_{1,2}) - (z_{1,2} - z_{r1,2})}(F_{f\max} + F_{fr1,2})\text{, for } z_{1,2} < z_{r1,2}. \tag{3.7}$$

The parameter $\alpha_{1,2}$ is given by the reference force-maximum friction force relation and its values range from -1 to 1.

The non-linearity of the secondary suspension model results, on the one hand, from the elastic force component developed in the mix coil spring – rubber and, on the other hand, from the component of friction force occurring in the rubber element.

4. The vehicle equations of motion

The vertical motion of the vehicle is described by both the equations of the vibration rigid modes in the carbody and bogie – bounce and pitch, and also by the equation of the first vertical bending mode of the carbody.

The general form of the carbody equation of motion is:

$$EI\frac{\partial^4 w_c(x,t)}{\partial x^4}+\mu I\frac{\partial^5 w_c(x,t)}{\partial x^4\partial t}+\rho_c\frac{\partial^2 w_c(x,t)}{\partial t^2}=\sum_{i=1}^{2}F_{zci}\delta(x-l_i)+\sum_{i=1}^{2}h_cF_{xci}\frac{\mathrm{d}\delta(x-l_i)}{\mathrm{d}x}\ , \tag{4.1}$$

where $\delta(.)$ is Dirac delta function, and F_{zci} and F_{xci} stand for the forces coming from the secondary suspension and from the traction longitudinal system

$$F_{zc1,2}=-2c_{zc1,2}\left(\frac{\partial w_c(l_{1,2},t)}{\partial t}-\dot z_{b1,2}\right)-2k_{zc1,2}\left[w_c(l_{1,2},t)-z_{b1,2}\right]-2c_v\left(\frac{\partial w_c(l_{1,2},t)}{\partial t}-\dot z_{v1,2}\right)+2F_{1,2} \tag{4.2}$$

$$F_{xc1,2}=2c_{xc}\left[h_c\frac{\partial^2 w_c(l_{1,2},t)}{\partial x\partial t}+h_b\dot\theta_{b1,2}\right]+2k_{xc}\left[h_c\frac{\partial w_c(l_{1,2},t)}{\partial x}+h_b\theta_{b1,2}\right]. \tag{4.3}$$

By applying the modal analysis method and considering the orthogonality property of the eigenfunction in the carbody vertical bending, the equation of motion (4.1) turns into three three-order differential equations with ordinary derivatives. These equations describe the movements of bounce, pitch and bending in the carbody:

$$\begin{aligned}&m_c\ddot z_c+2c_{zc}[2\dot z_c+2\varepsilon\dot T_c-(\dot z_{b1}+\dot z_{b2})]+2c_v[2\dot z_c+2\varepsilon\dot T_c-(\dot z_{v1}+\dot z_{v2})]+\\&+2k_{zc1}(z_c+a_c\theta_c+\varepsilon T_c-z_{b1})+2k_{zc2}(z_c-a_c\theta_c+\varepsilon T_c-z_{b2})-2(F_{f1}+F_{f2})=0\end{aligned} \tag{4.4}$$

$$\begin{aligned}&J_c\ddot\theta_c+2c_{zc}a_c[2a_c\dot\theta_c-(\dot z_{b1}-\dot z_{b2})]+2c_va_c[2a_c\dot\theta_c-(\dot z_{v1}-\dot z_{v2})]+\\&+2k_{zc1}a_c(z_c+a_c\theta_c+\varepsilon T_c-z_{b1})-2k_{zc2}a_c(z_c-a_c\theta_c+\varepsilon T_2-z_{b2})+\\&+2c_{xc}h_c[2h_c\dot\theta_c+h_b(\dot\theta_{b1}+\dot\theta_{b2})]+2k_{xc}h_c[2h_c\theta_c+h_b(\theta_{b1}+\theta_{b2})]-2a_c(F_{f1}-F_{f2})=0;\end{aligned} \tag{4.5}$$

$$\begin{aligned}&m_{mc}\ddot T_c+c_{mc}\dot T_c+k_{m2}T_c+2c_{zc}\varepsilon[2\dot z_c+2\varepsilon\dot T_c-(\dot z_{b1}+\dot z_{b2})]+2c_v\varepsilon[2\dot z_c+2\varepsilon\dot T_c-(\dot z_{v1}+\dot z_{v2})]+\\&+2k_{zc1}\varepsilon(z_c+a_c\theta_c+\varepsilon T_c-z_{b1})+2k_{zc2}\varepsilon(z_c-a_c\theta_c+\varepsilon T_c-z_{b2})+\\&+2c_{xc}h_c\lambda[2h_c\lambda\dot T_c+h_b(\dot\theta_{b1}-\dot\theta_{b2})]+2k_{xc}h_c\lambda[2h_c\lambda T_c+h_b(\theta_{b1}-\theta_{b2})]-2\varepsilon(F_{f1}+F_{f2})=0,\end{aligned} \tag{4.6}$$

where the below notations were introduced, based on the symmetry property of the eigenfunction $X_c(x)$

$$X_c(l_1)=X_c(l_2)=\varepsilon\ ;\ \frac{\mathrm{d}X_c(l_1)}{\mathrm{d}x}=-\frac{\mathrm{d}X_c(l_2)}{\mathrm{d}x}=\lambda\ . \tag{4.7}$$

The above equations will be added the 'hidden coordinate' equation of Maxwell model for the viscous component of the suspension force

$$c_v\left(\dot z_{v1,2}-\frac{\partial w_c(l_{1,2},t)}{\partial t}\right)+k_v(z_{v1,2}-z_{b1,2})=0, \tag{4.8}$$

which becomes after transformations

$$c_v[\dot{z}_{v1,2} - (\dot{z}_c \pm a_c\dot{\theta}_c + \varepsilon\dot{T}_c)] + k_v(z_{v1,2} - z_{b1,2}) = 0\,. \tag{4.9}$$

The relations (4.9) are still written as

$$c_v[2\dot{z}_c + 2\varepsilon\dot{T}_c - (\dot{z}_{v1} + \dot{z}_{v2})] = k_v[(z_{v1} + z_{v2}) - (z_{b1} + z_{b2})]\,; \tag{4.10}$$

$$c_v[2a_c\dot{\theta}_c - (\dot{z}_{v1} - \dot{z}_{v2})] = k_v[(z_{v1} - z_{v2}) - (z_{b1} - z_{b2})]\,. \tag{4.11}$$

The equations (4.10) and (4.11) will be replaced in the carbody equations of motion (4.4) – (4.6), changing into

$$\begin{aligned} &m_c\ddot{z}_c + 2c_{zc}[2\dot{z}_c + 2\varepsilon\dot{T}_c - (\dot{z}_{b1} + \dot{z}_{b2})] + 2k_v[(z_{v1} + z_{v2}) - (z_{b1} + z_{b2})] + \\ &+ 2k_{zc1}(z_c + a_c\theta_c + \varepsilon T_c - z_{b1}) + 2k_{zc2}(z_c - a_c\theta_c + \varepsilon T_c - z_{b2}) - 2(F_{f1} + F_{f2}) = 0 \end{aligned} \tag{4.12}$$

$$\begin{aligned} &J_c\ddot{\theta}_c + 2c_{zc}a_c[2a_c\dot{\theta}_c - (\dot{z}_{b1} - \dot{z}_{b2})] + 2k_v a_c[(z_{v1} - z_{v2}) - (\dot{z}_{b1} - \dot{z}_{b2})] + \\ &+ 2k_{zc1}a_c(z_c + a_c\theta_c + \varepsilon T_c - z_{b1}) - 2k_{zc2}a_c(z_c - a_c\theta_c + \varepsilon T_2 - z_{b2}) + \\ &+ 2c_{xc}h_c[2h_c\dot{\theta}_c + h_b(\dot{\theta}_{b1} + \dot{\theta}_{b2})] + 2k_{xc}h_c[2h_c\theta_c + h_b(\theta_{b1} + \theta_{b2})] - 2a_c(F_{f1} - F_{f2}) = 0\,; \end{aligned} \tag{4.13}$$

$$\begin{aligned} &m_{mc}\ddot{T}_c + c_{mc}\dot{T}_c + k_{m2}T_c + 2c_{zc}\varepsilon[2\dot{z}_c + 2\varepsilon\dot{T}_c - (\dot{z}_{b1} + \dot{z}_{b2})] + 2k_v\varepsilon[(z_{v1} + z_{v2}) - (z_{b1} + z_{b2})] + \\ &+ 2k_{zc1}\varepsilon(z_c + a_c\theta_c + \varepsilon T_c - z_{b1}) + 2k_{zc2}\varepsilon(z_c - a_c\theta_c + \varepsilon T_c - z_{b2}) + \\ &+ 2c_{xc}h_c\lambda[2h_c\lambda\dot{T}_c + h_b(\dot{\theta}_{b1} - \dot{\theta}_{b2})] + 2k_{xc}h_c\lambda[2h_c\lambda T_c + h_b(\theta_{b1} - \theta_{b2})] - 2\varepsilon(F_{f1} + F_{f2}) = 0\,. \end{aligned} \tag{4.14}$$

The equations describing the bounce and pitch motions in the bogies will be added to the previous relations:

$$\begin{aligned} &m_b\ddot{z}_{bi} + 2c_{zb}[2\dot{z}_{bi} - (\dot{\eta}_j + \dot{\eta}_{j+1})] + 2k_{zb}[2z_{bi} - (\eta_j + \eta_{j+1})] + \\ &+ 2c_{zc}(\dot{z}_{bi} - \dot{z}_c \mp a_c\dot{\theta}_c - \varepsilon\dot{T}_c) + 2k_{zci}(z_{bi} - z_c \mp a_c\theta_c - \varepsilon T_c) + 2k_v(z_{bi} - z_{vi}) + 2F_{fi} = 0\,; \end{aligned} \tag{4.15}$$

$$\begin{aligned} &J_b\ddot{\theta}_{bi} + 2c_{zb}a_b[2a_b\dot{\theta}_{bi} - (\dot{\eta}_j - \dot{\eta}_{j+1})] + 2k_{zb}a_b[2a_b\theta_{bi} - (\eta_j - \eta_{j+1})] + \\ &+ 2c_{xc}h_b[h_b\dot{\theta}_{bi} + h_c(\dot{\theta}_c \pm \lambda\dot{T}_c)] + 2k_{xc}h_b[h_b\theta_{bi} + h_c(\theta_c \pm \lambda T_c] = 0. \end{aligned} \tag{4.16}$$

The solving of the equations of motion is done numerically, by applying Runge-Kutta algorithm.

5. The results of the numerical simulations

This section describes the results of the numerical simulations based on which the influence of the nonlinear characteristics of the secondary suspension on the behaviour of vertical vibrations in the railway vehicle is analysed. The free vibrations behaviour, the steady-state harmonic behaviour of vibrations and of the

random vibrations behaviour are considered. Similarly, three reference points of the carbody are defined – at the centre and against the two bogies (against the bearing points of the carbody on the secondary suspension). The vibration behaviour at the carbody centre is the result of the overlapping between bounce and bending of the carbody. Against the two bogies, the carbody vibration is due to all three modes of vibration – bounce, pitch and bending of the carbody.

The parameters of the numerical model can be seen in Table 1, as representative for a passenger coach fitted with Y32 bogies.

Table 1

The parameters of the numerical model.

m_c = 34000 kg	L_c = 26.4 m	$2k_{zcc}$ = 0.66 MN/m	$2c_{zc}$ = 34.28 kNs/m
m_b = 3200 kg	$2a_c$ = 19 m; $2a_b$ = 2.56 m	$2k_{zcd}$ = 0.54 MN/m	$2c_{xc}$ = 50 kNs/m
m_{mc} = 35224 kg	h_c = 1.3 m; h_b = 0.2 m	$2k_v$= 250 kN/m	$4k_{zb}$ = 4.4 MN/m
k_{mc} = 88.998 MN/m	J_c = 1963840 kg·m^2	$2c_v$ = 4 kNs/m	$4c_{zb}$ = 52.21 kNs/m
c_{mc} = 53.117 kNm/s	J_b = 2048 kg·m^2	$2k_{xc}$ = 4MN/m	EI = 3.158·10^{9}Nm^2

For a first state, the behaviour of the free vibrations is looked at. The analysis will be about how the elastic characteristic with two-step variable stiffness influences the regime of the non-damped free vibrations. As for the initial conditions of the free vibrations, a vertical 10-mm displacement of the carbody is taken into account. Fig 5 shows the carbody vibration for a 10-sec time in the reference point at its centre. The vibration is found out not to be harmonic, due to the overlapping of the carbody eigenmodes of vibration – bounce and bending. It can be also noticed that the amplitudes of the expansion displacement are higher than of the compression's. Moreover, the periods corresponding to the expansion/compression displacements are not equal; the expansion's are longer than the compression's. For instance, when considering the average values for the 10 cycles, the amplitude of the displacement is 11.01 mm and the time 0.4418 s, for expansion. As for compression, the amplitude is 10.28 mm and the time 0.4144 s. These differences can be explained by a higher stiffness of the elastic element during compression, compared to expansion.

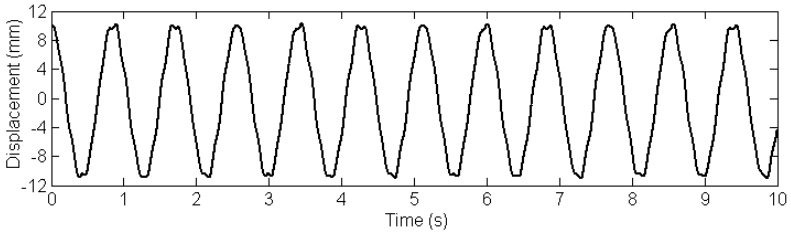

Fig. 5. The non-damped free vibrations of the carbody.

Another aspect to be analysed refers to the manner in which the damping coming from the friction in the rubber element in the secondary suspension

influences the regime of free vibrations in the carbody. To this purpose, only the component of dry friction will be considered, while the other damping coefficients are deemed null. The diagrams in Fig. 6 present how the free vibrations of the carbody are damped for various initial conditions – the displacement at the carbody centre of 5, 10 and 15 mm respectively, while having the maximum friction force of 100, 200 and 300 N. In the diagram, the displacements are normalized via the division by the value of the initial displacement. Firstly, the vibrations are noticed to have a slower damping when the initial displacement of the carbody increases. Secondly, the free vibrations of the carbody will be damped within a shorter period of time when the maximum friction goes up. Thirdly, the longer the initial carbody displacement, the lower frequency of vibrations, an aspect explained by the lowering in the stiffness of the rubber elements, due to the friction force component.

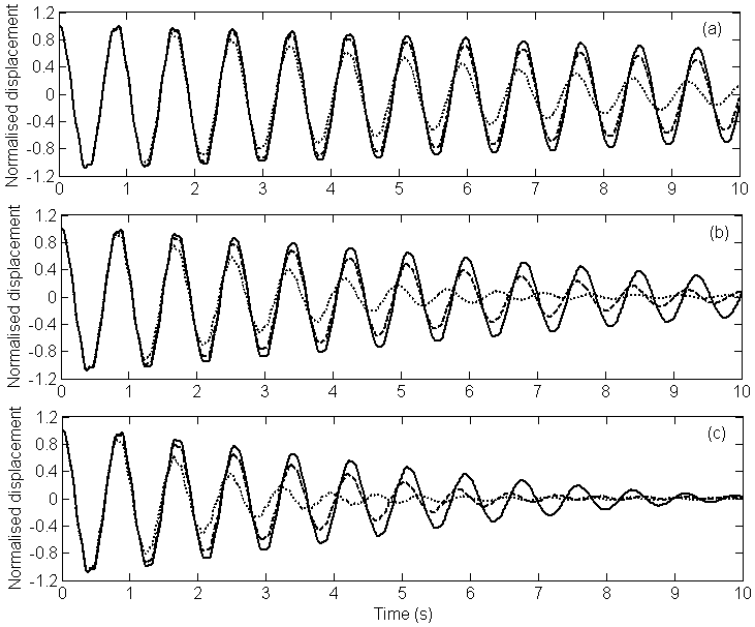

Fig. 6. The behaviour of the damped free oscillations:
(a) $F_{f\max}$ = 100 N; (b) $F_{f\max}$ = 200 N; (c) $F_{f\max}$ = 300 N; ——, initial displacement 15 mm; − − −, initial displacement 10 mm; · · · ·, initial displacement 5 mm.

As for the steady-state harmonic behaviour of vibrations, what interests most is the behaviour of carbody vibrations at the resonance frequencies of the vibration eigenmodes – 1.17 Hz – the frequency of the bounce vibrations; 8.20 Hz – the frequency of bending; 1.46 Hz – the frequency of the pitch vibrations (Dumitriu, 2015a). The vehicle is considered to travel at velocity of 200 km/h on a track with vertical irregularities of a sinusoidal shape with 1 mm in amplitude. The wavelength of the track vertical irregularities is thus selected so as the excitation

frequency correspond with the carbody eigenfrequency vibrations - 47.483 m for 1.17 Hz, 6.775 m for 8.20 Hz and 38.051 m for 1.46 Hz.

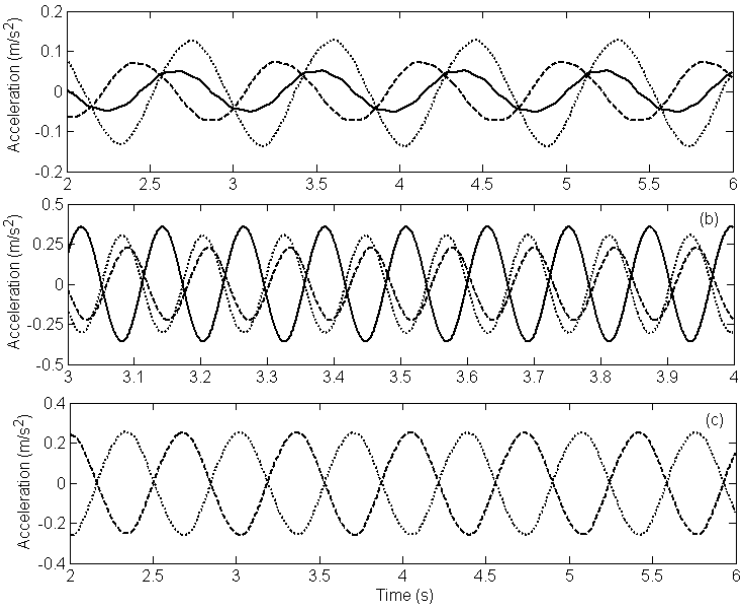

Fig. 7. The carbody acceleration in a permanent harmonic vibration behaviour:
(a) at 1.17 Hz; (b) at 8.20 Hz; (c) at 1.46 Hz;
—, at the carbody centre; − −, above the front bogie; · · · , above the rear bogie.

Fig. 7 features the vertical accelerations calculated in three reference points of the carbody for $F_{f\max}$ = 200 N. For the excitation frequency of 1.17 Hz, the highest acceleration is above the rear bogie and the lowest at the carbody centre. At 8.20 Hz, the maximum level of vibrations occurs at the carbody centre and the minimum level against the front bogie. For the excitation frequency of 1.46 Hz, the same level of vibrations will happen against the two bogies. If the excitation frequency is 1.17 Hz, the carbody motion is not harmonic and this is the result of the nonlinear characteristic of the secondary suspension. The above is also visible in Fig. 8, with the spectra of the vertical acceleration in the reference points of the carbody. Numerous harmonic components are present, as well as the one at 8.20 Hz whose frequency coincides with the carbody bending frequency.

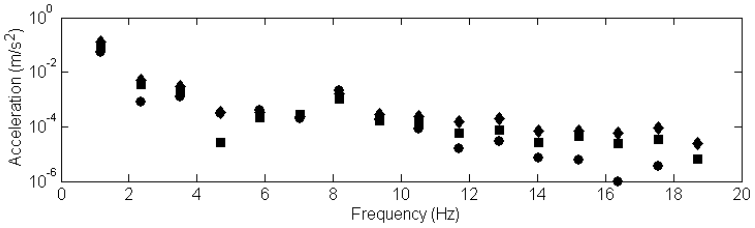

Fig. 8. Spectra of the carbody acceleration in a permanent harmonic vibration behaviour at 1.17 Hz:
●, at the carbody centre; ■, above the front bogie; ♦, above the rear bogie.

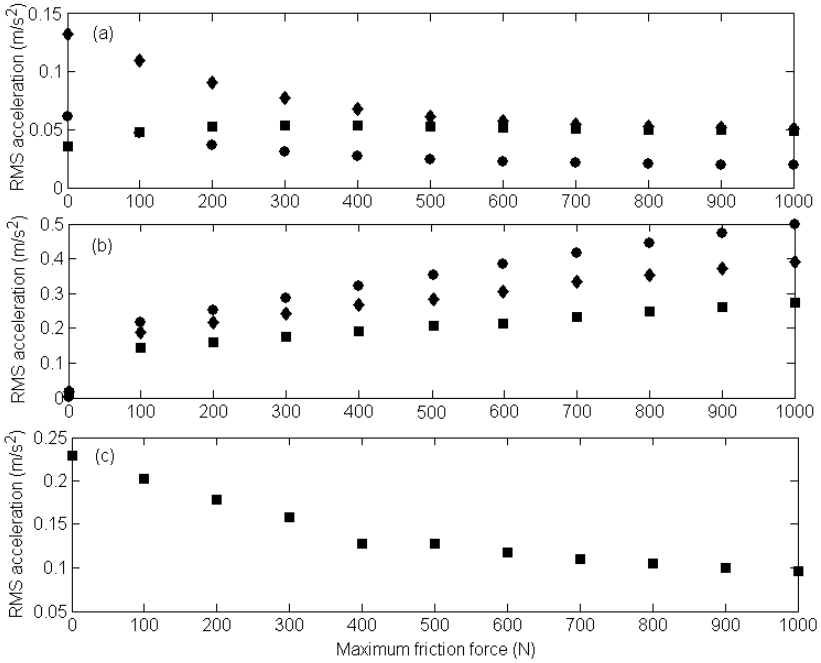

Fig. 9. Influence of the maximum friction force upon the steady-state harmonic vibrations behaviour:
(a) at 1.17 Hz, (b) at 8.20 Hz, (c) at 1.46 Hz;
●, at the carbody centre; ■, above the front bogie; ♦, above the rear bogie.

To examine the influence of the dry friction force upon the steady-state harmonic vibrations behaviour in the carbody, the diagrams in Fig. 9 are used, which introduces the RMS acceleration in the reference points of the carbody. The same values of the frequency induced by the track vertical irregularities are considered, namely 1.17 Hz (diagram (a)), 8.20 Hz (diagram (b)) and 1.46 Hz (diagram (c)), and different values of the maximum friction force within the range of 0 ... 1000 N. The influence of the friction force component can be seen to differently manifest as depending on the excitation frequency and the position of the reference point. For the frequency corresponding to the carbody bounce (1.17 Hz), the increase in the maximum friction force leads to an obvious decrease of the level of vibrations in the reference points at the carbody centre and against the rear bogie and less significant against the front bogie. Consequently, for this frequency, the increase of friction in the rubber element means a general decrease in the level of vibrations in the carbody. At the carbody bending frequency (8.20 Hz), a higher maximum friction force corresponds to a higher vertical acceleration in all the reference points of the carbody. In this situation, the stiffening of the secondary suspension triggers a higher value of the level of vibrations in the carbody. Should the excitation frequency coincide with the frequency of the

carbody pitch, the increase of the maximum friction force leads to a lower vibration level of the carbody in the reference points above the bogies.

Further on, the analysis refers to the influence of the friction force component upon the random vibrations regime in the carbody induced by the track vertical irregularities. Against each wheelset, the track vertical irregularities are described by a pseudo-stochastic function, written as (Dumitriu, 2015b)

$$\eta_{j,j+1}(x_{j,(j+1)}) = K_\eta f(x_{j,(j+1)}) \sum_{k=0}^{N} U_k \cos(\Omega_k x_{j,(j+1)} + \varphi_k), \text{ for } x_{j,(j+1)} > 0, \text{ for } j = 2i\text{-}1, \tag{5.1}$$

with, $x_1 = x = Vt$; $x_2 = x - 2a_b$, for $i = 1$; $x_3 = x - 2a_c$; $x_4 = x - 2a_b - 2a_c$, for $i = 2$, (5.2)

and $$K_\eta = \frac{\eta_{adm}}{\max\left| f(x_{j,(j+1)}) \sum_{k=0}^{N} U_k \cos(\Omega_k x_{j,(j+1)} + \varphi_k) \right|}, \tag{5.3}$$

where: K_η is a scaling coefficient of the amplitudes in the track lateral irregularities, η_{adm} is the maximum value of the track lateral irregularities as per UIC 518 Leaflet; $f(x_{j,(j+1)})$ is an adjustment function applied on the distance L_0, in the form of

$$f(x_{j,(j+1)}) = \left[6\left(\frac{x_{j,(j+1)}}{L_0}\right)^5 - 15\left(\frac{x_{j,(j+1)}}{L_0}\right)^4 + 10\left(\frac{x_{j,(j+1)}}{L_0}\right)^3 \right] H(L_0 - x_{j,(j+1)}) + H(x_{j,(j+1)} - L_0) \tag{5.4}$$

where $H(.)$ is the Heaviside's unit step function; U_k is the amplitude of the spectral component corresponding to the wave number Ω_k, and φ_k is the lag of the spectral component ‚k' for which a uniform random distribution is selected. The amplitude of each spectral component is established on the basis of the power spectral density of the track irregularities described in accordance with ORE B176 and the specifications included in the UIC 518 Leaflet regarding the track geometrical quality described by the quality levels QN1 and QN2.

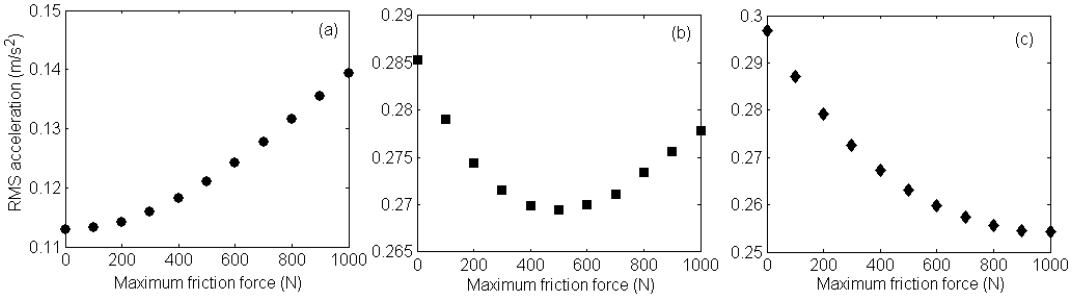

Fig. 10. Influence of the maximum friction force upon the random vibrations regime: (a) at the carbody centre; (b) above the front bogie; (c) above the rear bogie.

Fig. 10 displays the influence of the friction force component upon the random vibrations behaviour in the carbody, evaluated as based on the RMS acceleration – an appreciation criterion for the ride quality (UIC 518 Leaflet, 2009), at the velocity of 200 km/h on a QN2 quality track. Former, the highest level of vibrations is noticed in the reference points above the two bogies. Latter, the influence of the friction force has a different manifestation, depending on the position of the reference point. At the carbody centre, the increase in the friction force means a higher RMS acceleration. In the reference point located above the front bogie, the RMS acceleration has a minimum for $F_{f\max}$ = 500 N. Against the rear bogie, the level of vibrations goes down along with the going up of the friction force.

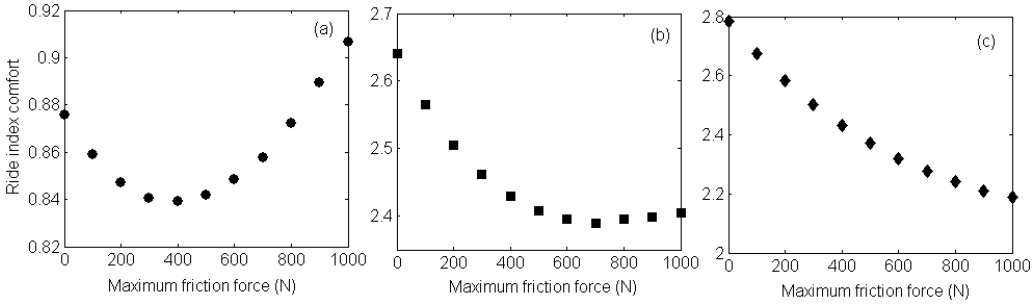

Fig. 11. Influence of the maximum friction force upon the ride comfort:
(a) at the carbody centre; (b) above the front bogie; (c) above the rear bogie.

The influence of the friction force component is also visible on the ride comfort, as evaluated on the ride index comfort (ENV 12299, 1997), as seen in Fig. 11. The influence of the friction force component depends on the position of the reference point of the carbody in this case, as well.

At the carbody centre and against the front bogie, the best comfort index can be obtained for a certain value of the friction force: $F_{f\max}$ = 400 N – at the carbody centre and $F_{f\max}$ = 700 N – against the front bogie. Against the rear bogie, the comfort index lowers along with the increase of the friction force. It is worth mentioning that the level of vibrations is smaller at the carbody centre and higher against the two bogies, irrespective of the value in the friction force.

6. Conclusions

The paper is a parametric study aiming to analyse the influence of the nonlinear characteristics of the secondary suspension upon the behaviour of vertical vibrations of the vehicle carbody in three reference points – at the carbody centre and against the two bogies. The model of the secondary suspension herein includes two nonlinear aspects derived from the component of the elastic force coming from the mix coil spring – rubber, on the one hand, and from the

component of the dry friction force developed in the rubber element, on the other hand.

The study is based on the results from the numerical simulation underlying a rigid-flexible coupled model of the vehicle, where the carbody is modelled as Euler-Bernoulli beam. The free vibrations behaviour, the steady-state harmonic behaviour of vibrations and of the random vibrations behaviour have been taken into account.

The analysis has also applied to the manner in which the elastic characteristic with a two-step variable stiffness influences the behaviour of the non-damped free vibrations. The amplitudes and the time periods of the displacements of the carbody are not equal, due to the higher stiffness of the elastic component during compression, compared with expansion. Upon examining the influence of the dry friction force upon the behaviour of free vibrations, the conclusion was that the damping of the nonlinear system depends on the amplitude and frequency of the free vibrations.

Based on the study of the vibrations regime of the carbody generated by the track vertical irregularities in harmonic shape, the influence of the friction force was visibly different in its manifestation, depending on the excitation frequency. Therefore, the increase in the maximum friction force at the excitation frequencies corresponding to the carbody bounce and pitch leads to a reduced level of vibrations in the carbody. On the contrary, higher friction in the rubber element means increase in the level of vibrations in all the reference points of the carbody, at the excitation frequency corresponding to the carbody bending.

The analysis of the random vibrations behaviour has made obvious the effect of the friction component upon the level of vibrations in the carbody, in terms of ride quality and ride comfort. The influence of the friction component has been proven to manifest differently in the reference points of the carbody. Generally speaking, a higher friction force triggers an improvement in the ride quality and ride comfort in the reference points against the bogies, points to be considered critical when dealing with the level of vibrations in the carbody.

Acknowledgments

This work has been funded by University Politehnica of Bucharest, through the "Excellence Research Grants" Program, UPB – GEX - 2016. Research project title: *Research on developing mechanical and numerical models for the virtual evaluation of the dynamic performances in the railway vehicles* (in Romanian). Contract number: 48/26.09.2016.

R E F E R E N C E S

[1] *Berg M.*, 1997, A model for rubber springs in the dynamic analysis of rail vehicles, Proceedings of the Institution of Mechanical Engineering, Part F: Journal of Rail and Rapid Transit, **211**, 95-108.

[2] *Berg M.*, 1998, A non-linear rubber spring model for rail vehicle dynamics analysis, Vehicle System Dynamics, **30**, 197-212.
[3] *Bruni S., Vinolas J., Berg M., Polach O., Stichel S*., 2011, Modelling of suspension components in a rail vehicle dynamics context, Vehicle System Dynamics, **49**, 7, 1021–1072.
[4] *Cheli F., Corradi R.*, 2011, On rail vehicle vibrations induced by track unevenness: Analysis of the excitation mechanism, Journal of Sound and Vibration, **330**, 3744–3765.
[5] *Diana G., Cheli F., Collina A., Corradi R., Melzi S*., 2002, The development of a numerical model for railway vehicles comfort assessment through comparison with experimental measurements, Vehicle System Dynamics, **38**, 3, 165- 183.
[6] *Dumitriu M*., 2016, A nonlinear model of mix coil spring – rubber for vertical suspension of railway vehicle, Archive of Mechanical Engineering, **LXIII**, 1, 125-142.
[7] *Dumitriu M*., 2015a, Analysis of the dynamic response in the railway vehicles to the track vertical irregularities. Part II: The numerical analysis, Journal of Engineering Science and Technology Review, **8**, 4, 32 – 39.
[8*] Dumitriu M*., 2015b, Method to synthesize the track vertical irregularities, Scientific Bulletin of the "Petru Maior" University of Tîrgu Mureş, **11**, 2, 17-24.
[9] *Eickhoff B.M., Evans J.R., Minnis A.J.*, 1995, A review of modelling methods for railway vehicle suspension components, Vehicle System Dynamics, **24**, 6–7, 469–496.
[10] ENV 12299, 1997, Railway applications ride comfort for passengers measurement and evaluation.
[11] *Evans J., Berg M.*, 2009, Challenges in simulation of rail vehicle dynamics, Vehicle System Dynamics, **47**, 1023–1048.
[12] *Funfschilling C., Perrin G., Kraft S.*, 2012, Propagation of variability in railway dynamic simulations: Application to virtual homologation, Vehicle System Dynamics, **50**, 245–261.
[13] *Jönsson L.O., Nilstam N., Persson I.*, 2008, Using simulations for approval of railway vehicles, Vehicle System Dynamics, **46**, 869–881.
[14] *Mazilu T*., 2009, On the dynamic effects of wheel running on discretely supported rail**,** Proceedings of the Romanian Academy, Series A: Mathematics, Physics, Technical Sciences, Information Science, **10**, 3, 269-276.
[15] *Mazilu T.*, 2010, Prediction of the interaction between a simple moving vehicle and an infinite periodically supported rail-Green's functions approach, Vehicle System Dynamics, **48**, 9, 1021-1042.
16] ORE B 176, 1989, Bogies with steered or steering wheelsets, Report No. 1: Specifications and preliminary studies, Vol. 2, Specification for a bogie with improved curving characteristics.
[17] *Schupp G.*, 2003, Simulation of railway vehicles: Necessities and applications, Mechanics Based Design of Structures and Machines, **31**, 3, 297–314.
[18] UIC 518 Leaflet, 2009, Testing and approval of railway vehicles from the point of view of their dynamic behaviour – Safety –Track Fatigue – Ride Quality.
[19] *Young T.H., Li C.Y.*, 2003, Vertical vibration analysis of vehicle/imperfect track systems, Vehicle System Dynamics, **40**, 5, 329–349.